Nuclear Instruments and Methods in Physics Research A 598 (2009) 23–30

Contents lists available at ScienceDirect

Nuclear Instruments and Methods in Physics Research A

journal homepage: www.elsevier.com/locate/nima

Review of beam energy measurements at VEPP-4M collider KEDR/VEPP-4M ☆

V.E. Blinov, A.V. Bogomyagkov, N.Yu. Muchnoi, S.A. Nikitin, I.B. Nikolaev, A.G. Shamov, V.N. Zhilich *

Budker Institute of Nuclear Physics, Novosibirsk, Russia

ARTICLE INFO

Available online 23 August 2008

Keywords:
Beam energy measurement
Energy calibration
Depolarization technique
Compton scattering

ABSTRACT

An accurate knowledge of the colliding beam energies is essential for the current experiments with the KEDR detector at the VEPP-4M collider. Now the experimental activity is focused on the measurements of τ lepton mass and parameters of narrow resonances of the ψ-family in the c.m.energy range of 3.0–4.0 GeV. Two complementary approaches are used for the beam energy measurements. The resonant spin depolarization technique (RD) provides an accuracy about 1–3 keV for the instantaneous beam energy value, but requires a special regime of the collider. Between calibrations the interpolation procedure is used providing the accuracy of 6–10 keV for the J/ψ, ψ(2s) and 15–30 keV for the τ lepton mass determination experiments.

Another approach allows to calculate beam energy via the maximum energy of backscattering laser photons. The Compton BackScattering (CBS) monitor allows continuous on-line monitoring of the beam energy with accuracy about 150 keV, which is critical during the τ lepton mass measurement. The statistical error for a 1 h period is about 100 keV, the present systematic error is 50–70 keV.

© 2008 Published by Elsevier B.V.

1. Introduction

Since 2002 experiments are performed with the universal magnetic detector KEDR [1] at the electron–positron collider VEPP-4M [2] at BINP. The VEPP-4M collider consists of the booster ring VEPP-3 with energy from 500 to 2000 MeV and the main ring operating in the beam energy range from 1 to 5.5 GeV. The physics program of the detector is focused on the study of ψ-, ϒ-mesons and γγ-physics. The goal of the first series of the experiments was precise mass measurements of J/ψ, ψ(2s), ψ(3s), D mesons and τ lepton. The resonant depolarization technique [3] was used for precise instantaneous energy calibration. Continuous energy measurements were performed by determination of the utmost energy of the γ-quanta obtained from the Compton BackScattering (CBS) of laser photons against the electron beam [4]. The present paper describes both methods, realization characteristics, achieved precision in experiments with the KEDR detector at the VEPP-4M collider.

2. Resonant depolarization technique

The resonant depolarization (RD) technique was proposed at BINP in 1975 [5,6] and used in precise mass measurement of various particles: ϕ [7], $K^{\pm}$ [8], J/ψ and ψ(2s)-mesons [9], ϒ, ϒ(2s)-, ϒ(3s) mesons [10–14], Z-boson [15]. The relative accuracy of mass measurements in these experiments was $10^{-4}-10^{-5}$. The method itself is similar to the phenomena of electron or nuclear magnetic resonances. Spin of the electron traveling in the magnetic field precesses around the direction of the field. In a storage ring with a flat orbit without torsion the spin precession frequency Ω depends on the Larmor revolution frequency of the particle ω_0 and Lorentz factor γ:

$$\Omega = \omega_0\left(1+\gamma\frac{\mu'}{\mu_0}\right) \tag{1}$$

where μ'/μ_0 is the ratio of anomalous and normal parts of electron magnetic momentum known with a relative accuracy of 3.3×10^{-9} [16]. The average particle revolution frequency ω_0 is completely determined by frequency of the accelerating RF field and could be set and measured with high accuracy. Thus, energy measurement is reduced to spin frequency measurement Ω, which is convenient to represent in units of revolution frequency and in the coordinate basis related to the particle velocity vector: $\nu=\gamma\mu'/\mu_0$. In order to measure spin precession frequency, resonant influence of an external electromagnetic field on spin motion is used [5,6]. Hence, the spin precession frequency is

☆ This work is supported by Russian Foundation for Basic Research, Grants 07-02-00426-a, 07-02-01162-a, 07-02-00816-a, 08-02-00258-a, 08-02-00251-a and in part by the Presidential Grant for Scientific School NSh-5655.2008.2.

* Corresponding author.
E-mail address: zhilich@inp.nsk.su (V.N. Zhilich).

0168-9002/$ - see front matter © 2008 Published by Elsevier B.V.
doi:10.1016/j.nima.2008.08.078

measured at the moment of depolarization during a scan of the external electro-magnetic field frequency. Depolarization happens when the resonant condition is satisfied:

$$\omega_d \pm \Omega = k\omega_0 \quad (2)$$

where k is the any integer, ω_d the electromagnetic field frequency. The external electromagnetic field could be created in the form of the alternating longitudinal magnetic field or transverse TEM wave propagating against the beam with the magnetic field direction perpendicular to the polarization vector. The moment of depolarization is detected by the process which cross-section depends on the polarization degree.

Since there is an energy spread in the beams of the electron–positron collider, the instantaneous spin tune spread σ_ν is proportional to the energy deviation RMS σ_E: $\sigma_\nu/\nu = \sqrt{2}\sigma_E/E \approx 10^{-3}$.

There is one more characteristic of the spin frequency distribution in a beam—an intrinsic spin line width ($\varepsilon_\nu \ll \sigma_\nu$) which corresponds to averaging of the spin motion over synchrotron and betatron oscillations. The synchrotron oscillations yield a shift and widening of the spin line at the level $\Delta\Omega/\Omega \sim 10^{-8}$. Practically, the spin line width is determined by nonlinear effects of particle motion in the storage ring fields. The RD process is very slow as compared with any period of the orbital motion. It allows us to consider the spin frequency spectrum as a set of narrow isolated lines and to measure the spin frequency with an error much smaller than the instantaneous spin tune spread σ_ν. The spin frequency spectrum due to the modulation effect of the orbital motion consists of the main and sideband lines. The synchrotron oscillations sideband lines are distant from the main line at the value $\nu_{synch} \simeq 0.01$ which is equivalent to a 4.4 MeV bias for the VEPP-4M. Therefore, a special care has to be taken to avoid depolarization at the synchrotron sideband line. The sidebands from the betatron oscillations are about 200 MeV apart from the main line and practically never cross during the usual frequency scan.

Pulsations of the guiding field will change the revolution frequency as well as the energy of the particles. Therefore, there will be additional sidebands in the spin precession frequency spectrum at the magnetic field pulsation frequencies. These side bands might be very close to the main line, for instance a 50 Hz pulsation is only 26 keV away from the main line. Hence, one needs to keep an amplitude of pulsations small enough (<15 ppm) in order not to depolarize the beam at the wrong frequency and keep the depolarizer amplitude as small as possible (so depolarization does not happen at sidebands but is still possible at the main line).

The spread of the particles horizontal trajectories in the presence of the sextupole fields in the accelerator will be responsible for associated spin tune width. The half-width (which is responsible for a bias during the beam energy measurement) is estimated to be $\varepsilon_\nu = \Delta\nu/\nu \approx 5 \times 10^{-7}$ (≈ 1 keV). This effect is the primary source of uncertainty of the spin tune measurements.

2.1. Touschek polarimeter

Various methods for measuring of the electron/positron beam polarization in the storage rings have been developed and used at BINP during last 30 years [17,18,20]. The most effective of them applied to the low energy range of VEPP-4M including the J/ψ, ψ(2s) peaks as well as τ production threshold is the observation of spin dependence in the intra-beam (Touschek) scattering. The cross-section of the intra-beam scattering of polarized electrons is smaller than for unpolarized particles. The detected counting rate of scattered electrons will experience a jump at the moment of depolarization proportional to the squared polarization degree P^2. Numerous variations of beam parameters change the counting rate hampering observation of the true moment of depolarization. Therefore, scattered electrons are detected from two nearly equal electron bunches separated by half a turn, one beam being polarized and the other one not. In such an approach the relation $1 - N_2/N_1$ will experience a jump at the moment of depolarization, where N_1 and N_2 are the counting rates of the polarized and unpolarized beams, respectively (Fig. 1). The ratio N_2/N_1 was found to be less sensitive to the change of the beam parameters than any of N_i.

The polarimeter system consists of several groups of scintillator counter installed in the technical and experimental section of the VEPP-4M. In Fig. 2 they are marked as DC—distributed counters. Every group consists of a pair of scintillation counters on opposite sides of the vacuum chamber in a horizontal plane. Each counter could be moved inside the aperture in order to optimize a

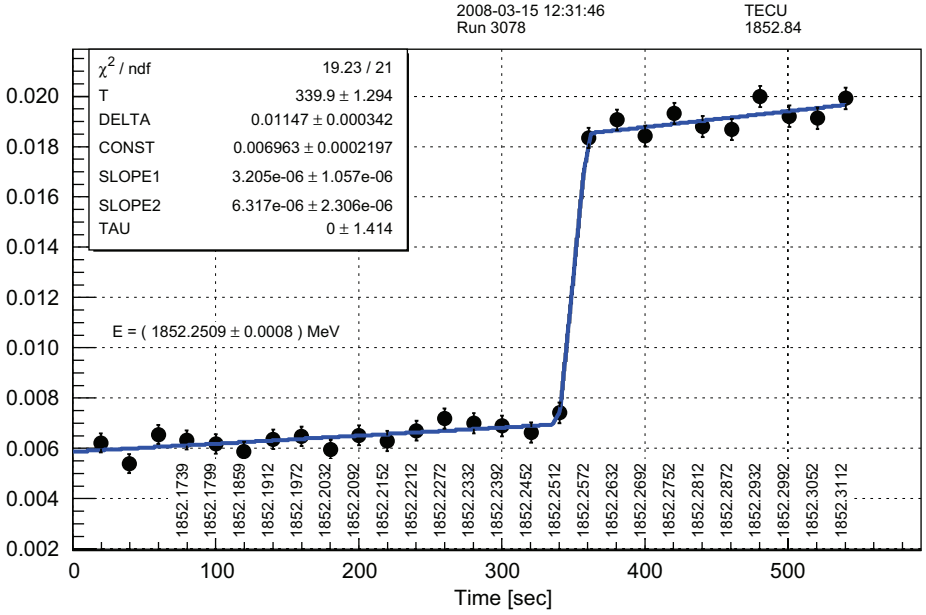

Fig. 1. The ratio of counting rates from polarized and unpolarized beams during depolarization. The statistical error for Ebeam is 0.8 keV.

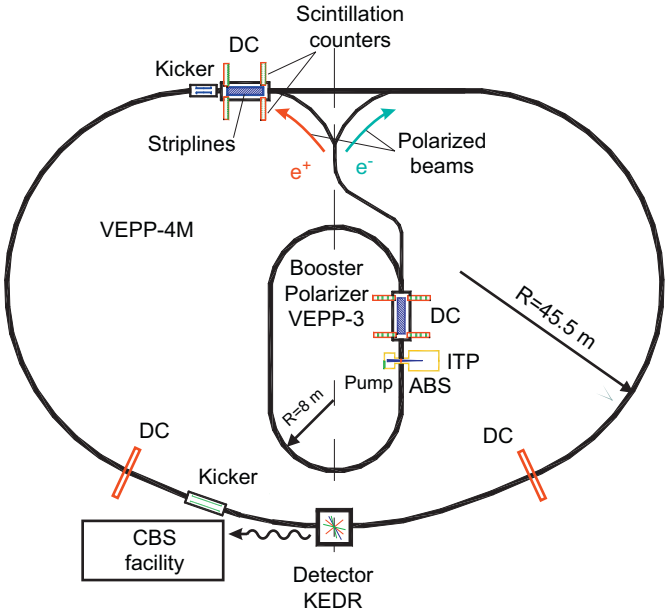

Fig. 2. VEPP-4M layout.

counting rate. Since the trajectories of Touschek pair electrons lie symmetrically on each side of the closed orbit, usage of the twofold coincidence for counter pulses allows to suppress the beam background. At the present time the counting rate of the polarimeter system reaches 1 MHz at the beam current of 2−4 mA and at 1 cm distance from the counters to the beam (at this distance the beam life time is not yet significantly affected). The jump of the ratio N_2/N_1 is 2.5−3.5% in the energy range 1.5−1.8 GeV being in the good agreement with the calculation (at $P = 80\%$).

2.2. Depolarizer

The two matched striplines of the VEPP-4 kicker (Fig. 2) are used to create a TEM wave propagating towards the beam. The signal source is a frequency synthesizer with a minimal frequency step of 0.35 mHz. For VEPP-4M, 1 keV in the beam energy scale corresponds to 1.85 Hz in the depolarizer frequency f_d. The power wide-band amplifier can provide an amplitude of the voltage across strip lines up to $U_d \approx 200$ V. The rate τ_d^{-1} of forced depolarization with the transverse field crucially depends on the absolute value of the spin response function $|F^\nu|$ [17] at the place of the depolarizer location: $\tau_d^{-1} \propto U_d^2 \cdot |F^\nu|^2/\Delta f_d$. Δf_d is the depolarizer frequency line width which we artificially spread via the computer controlled synthesizer with the aim to avoid a depolarization at the weak sideband resonances. For VEPP-4M, the design depolarization time τ_d is about 2 s at $E = 1550$ MeV with $U_d \approx 15$ V, $\Delta f_d \approx 4$ Hz, $|F^\nu|^2 = 130$. The typical depolarizer parameters in the J/ψ experiment were the rearrangement step of the depolarizer frequency 2 Hz; the band width (due to modulation at the frequency $f_m = 2$ Hz $\Delta f_d = 4$ Hz; the voltage amplitude 12 V; the average rate of the frequency rearrangement 0.2 Hz/s. The corresponding accuracy in the instantaneous energy determination is $\Delta E \approx \pm 1$ keV.

2.3. Calibration of particle absolute energy

In the energy range of J/ψ, ψ(2s)-mesons and τ lepton the VEPP-3 booster storage ring serves a source of polarized beams for VEPP-4M (Fig. 2). Due to Sokolov–Ternov effect the electron/positron beams become polarized in VEPP-3 with the characteristic time $\tau_p \approx 80$ min at $E = 1550$ MeV (J/ψ) and $\tau_p \approx 30$ min at $E = 1840$ MeV (ψ(2s)). The very large polarization time in the VEPP-4M ($\sim 10^2$ h) does not allow to obtain polarized beams immediately in the main ring. The polarized beam is then injected in the VEPP4-M and about 10 min later an unpolarized beam is added as a second bunch. The regime of the VEPP-4M during energy calibration is slightly different from the one with luminosity (all electrostatic separation is off). This is done to minimize possible errors associated with electron and positron energy differences.

Formula (1) allows to calculate beam energy after measurement of the spin precession frequency only for an ideal accelerator with an absolutely flat orbit. Vertical orbit distortions, local orbit bumps, errors of detector longitudinal field compensation are responsible for bias of the beam energy from a calculated one. Applied corrections and associated uncertainties have been described in Refs. [19,21,22]. One of the RD calibration results is shown in Fig. 1. The statistical error for the beam energy is 0.7 keV. The total correction for the orbit distortion comprises $\Delta E \simeq 3-5$ keV.

Due to the depolarizer (Section 2) and the spin line (Section 2.2) widths the measured beam energy is biased with the value about ±1.5 keV. The sign is determined by the frequency scan direction—up or down. This bias can be measured and corrected with two opposite scans which can be done with the same beam within short time.

The total systematic error for instantaneous beam energy is about 2 keV [22]. The whole process of energy calibration by RD consumes about 2 h and was performed once a day for $J/\psi, \psi'$ scans and once for a few day for τ, ψ'' case. Since 2002 more than 1500 calibrations have been performed.

2.4. Assignment of energy to data acquisition runs

The energy calibration technique described above does not allow the energy calibration during the data acquisition. Rather large energy variations can occur between the calibrations, therefore some procedure is required to assign the energy to data acquisition runs using the results of the RD calibration.

In the experiments [11–13,15] the guide field measurements were used to calculate the beam energy supposing that

$$E_{\text{beam}} = \alpha_H \cdot H_{\text{NMR}} \tag{3}$$

with the field strength H_{NMR} measured in a reference dipole powered in series with the main ring magnets and the α_H is a coefficient determined using nearby calibrations. The simple relation (3) implies the absence of orbit variations. The direct orbit measurements are usually not accurate and comprehensive enough to be used for a correction of the α_H value. In VEPP-4M there are 10 independent bending magnet power supplies, 60 radial correctors and only 54 beam position monitors. However, the empiric improvement of Eq. (3) is possible using observable parameters such as magnet and machine tunnel temperatures, magnet currents and the explicit time dependence to take into account the parameters which cannot be observed.

In the J/ψ and ψ(2s) mass experiment [22] the following extension of (3) was suggested:

$$\begin{aligned} E_{\text{beam}} = {} & \alpha_H \cdot H_{\text{NMR}} \cdot (1 + \alpha_T \cdot (T_{\text{ring}} - T_{\text{NMR}})) \\ & \times f(T_{\text{ring}}, T_{\text{cool}}, T_{\text{tunnel}}) + A(t) \cdot \cos\left(\frac{2\pi t}{\tau_{\text{day}}} - \varphi(t)\right) \\ & + \delta E_{\text{on}} \cdot \exp\left(-\frac{t_{\text{on}}}{\tau_{\text{on}}}\right) + \delta E_{\text{cycle}} \cdot \exp\left(-\frac{t_{\text{cycle}}}{\tau_{\text{cycle}}}\right) + E_0(\Delta i, t) \end{aligned} \tag{4}$$

where T_{NMR} is the temperature of the reference dipole, T_{ring} and T_{cool} are the average values of the ring and the cooling agent (air or water) temperatures, the temperature T_{tunnel} is measured in some depth of the machine tunnel walls; t is current time, t_{on} and t_{cycle} denote time elapsed since the last switching of the collider and the last magnetization cycle, respectively.

The α_H, α_T, δE_{on}, δE_{cycle}, τ_{on} and τ_{cycle} are free parameters to be determined by the fit of all energy calibrations performed in a certain operating mode of the collider. The simplest (linear or step-like) functions $f(T)$, $A(t)$, $\varphi(t)$ and $E_0(\Delta i, t)$ have additional free parameters.

In this parameterization the difference of the reference dipole and the ring magnet conditions is accounted. Also the variations of the ring circumference and the corresponding shift of the orbit position relative to the magnets due to temperature variations is accounted partially by the linear function $f(T)$. The significance of this effect at the VEPP-4M is known since 1982 [10]. The residual temperature effect is described by the day-to-night oscillations. In general, the amplitude A and the phase φ are not constant due to season variations in properties of the ground surrounding the machine tunnel. The fitted value of A depends on the quality of the tunnel temperature monitoring. During the experiment [22] it was not monitored at all.

The exponential terms introduce the magnetic field relaxation; ignoring this effect results in a bias in the parameters α_H, α_T, etc. The term $E_0(\Delta i, t)$ serves to take into account the energy variation due to adjustments of the current Δi in some machine elements and thus to increase the number of calibrations which can be fitted together.

The results of the energy fit for May 2002 are illustrated in Fig. 3. Fourteen free parameters are used to fit 28 points shown in the figure. The value of the χ-squared per degree of freedom is employed to estimate the (mean) error of the energy interpolation by requiring $\chi^2/N_{dof} = 1$.

The appearance of strong day-to-night oscillations (the 100th day of the experiment on (Fig. 3) and their further growth (between 107th and 110th days) can be probably explained by the change of the thermo-mechanical properties of the ground surrounding the VEPP-4M tunnel. These properties can change abruptly at the moment when the melting front reaches the tunnel (in Novosibirsk it occurs in May). According to the χ^2 criterion, the sudden growth of the oscillation amplitude on the 100th day is much more probable than the gradual one.

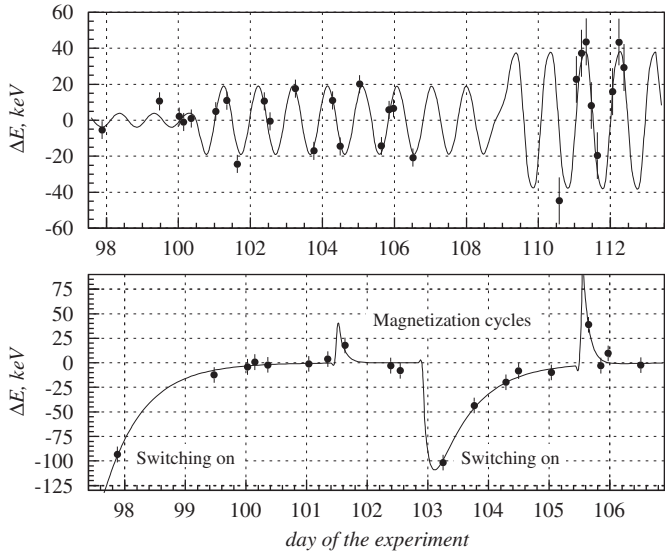

Fig. 3. The example of the beam energy behavior. Upper—periodic dependence on time, lower—aperiodic energy dependence on time due to switching on the ring and the magnetization cycles. All dependences but presented ones are taken into account in ΔE, the error bars show the mean deviation from the fit.

During the whole experiment [22] (218 calibrations) the quasi-statistical accuracy of the interpolation varies from 6 to 8 keV. Various choices of the functions $f(T)$, $A(t)$ and $\varphi(t)$ was tried to estimate the systematic uncertainties of the resulting J/ψ and ψ(2s) mass values.

To apply the parameterization (4) in its full form, the large number of calibrations is required without essential change of the collider operating mode. In the measurements of the ψ(2s), D mesons and τ lepton masses [23,24] the simplified forms of Eq. (4) were employed at the relatively short time intervals. The number of free parameters varies from 4 to 7. The interpolation accuracy achieved is 10−15 keV for the narrow resonance scans and 15−30 keV for the τ-threshold and ψ(2s) scans. The interpolation of RD results at the τ-threshold is compared with the alternative method of the beam energy determination in Fig. 7 shown below.

3. CBS monitor

The kinematics of the Compton scattering can be easily derived from the four-momenta conservation low. The energy spectrum of scattered photons is rather flat and has a sharp edge at maximal energy ω_{max}. For a head-on collision of the photon with energy ω_0 with the electron with energy E the maximum energy of the backscattered photons is given by

$$\omega_{max} = \frac{E^2}{(E + me^2/4\omega_0)} \simeq 4\gamma^2\omega_0 \tag{5}$$

where m_e is an electron mass, $\gamma = E/m_e$. There is a correlation between photon energy and its scattering angle $\omega \simeq \omega_{max}/(1 + (\gamma\theta)^2)$. High-energy photons form a narrow cone along an initial electron momentum.

One can obtain the absolute value of the electron energy E by measuring ω_{max}:

$$E = \frac{\omega_{max}}{2}\left(1 + \sqrt{1 + \frac{m^2}{\omega_0\omega_{max}}}\right). \tag{6}$$

If the beam has an energy spread of σ_E, the spectrum edge would get smeared to $\sigma(\omega)/\omega \approx 2\sigma_E/E$. Thus, this approach allows to measure the beam energy spread as well.

The accuracy of the beam energy calculation is limited by the accuracy of ω_{max}, since the energy of the laser photons can be determined with a relative accuracy of 10^{-5}–10^{-7}.

The CBS approach for beam energy measurements was previously realized at the BESSY-I and BESSY-II synchrotron radiation facilities [25].

In our case the CBS monitor has been originally designed to monitor VEPP4-M energy during experiment on the precise measurement of the τ lepton mass. The τ mass is derived from the τ production rate near the reaction threshold. The expected accuracy for the τ mass is about 150 keV, then the accuracy for beam energy measurement of 75 keV is rather satisfactory. Due to very small statistics of detected τ lepton decays near threshold even single event with an energy shift of 0.5 MeV can increase an experimental error by a factor of 2. Therefore, unexpected energy shifts which sometimes happen due to technical problems in the magnetic system are very undesirable. The on-line beam energy

monitoring with an accuracy about 100 keV is quite adequate for this task.

3.1. Experimental setup

The following equipment was selected to be used for this approach.

- The carbon dioxide laser (GEM Select 50 by COHERENT Inc.) works at the wavelength $\lambda = 10.591035\,\mu m$ ($\omega_0 = 0.11706522$ eV). It provides ω_{max} in the range of 4–7 MeV. The average energy of laser photons is stable at the level of $\Delta\omega_0/\omega_0 \simeq 10^{-7}$. The continuous power of laser radiation is about 30 W.
- The High Purity Germanium (HPGe) detector was found to be the best calorimeter for measuring the energy spectrum of backscattered photons. The Canberra model GC2518 detector is used with the active volume of 120 cm^3. The efficiency of total absorption in the detector is about 5% for 6 MeV photons. Its internal energy resolution is about $(0.6 + 0.2\omega\,[\text{MeV}])$ keV. In the real case the pile-up noise contributes additional (1–3) keV.
- The HPGe detector energy scale is calibrated with the well-known sources of γ-radiation in the range of 0.5–2.7 MeV. The scale extrapolation to ω_{max} is necessary.

The facility layout is shown in Fig. 4. The laser light enter the VEPP-4M vacuum chamber through the system of mirrors, zooming lenses and infrared transparent ZnSe window. It interacts with the electron beam in the 12 m straight section of the VEPP-4M collider. The backscattered high-energy photons propagate toward the HPGe detector. The laser is focused near the center of the KEDR detector with an effective length of ±200 cm. The spot size is 1–2 mm. The transverse beam size is about $0.35 \times 0.01\ mm^2$. The expected intensity of scattered photons is about 30 kHz for 1 W of laser power but only an ~2% fraction really contributes to the energy measurement.

3.1.1. Measurement procedure

During KEDR experiments in 2005–2007 the CBS monitor was operating continuously. The energy scale and resolution of the HPGe detector was controlled by calibration peak positions and widths. The calibration γ-sources (^{60}Co, ^{137}Cs, ^{24}Na, ^{228}Th) were placed around the HPGe detector giving the counting rate about 1 KHz. The counting rate of Compton photons above 3 MeV threshold was 1–5 kHz. The detector was usually set to acquire photon spectra of 5×10^6 counts, which took about 10–60 min. Each spectrum provides self-sufficient information for the beam energy measurement. The spectrum example for $E \approx 1580$ MeV is shown in Fig. 5.

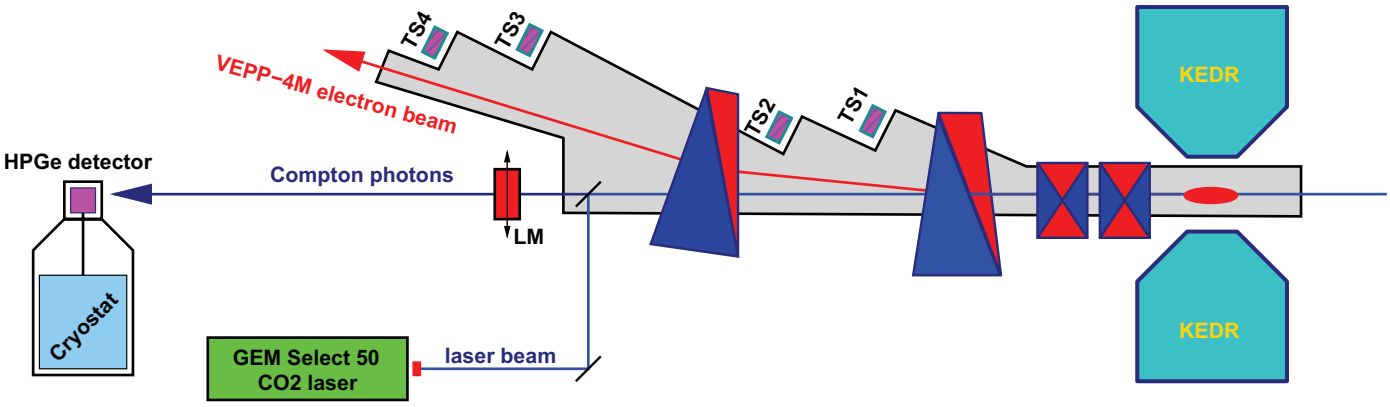

Fig. 4. Experimental setup. A distance of the HPGe detector from the interaction point is about 16 m.

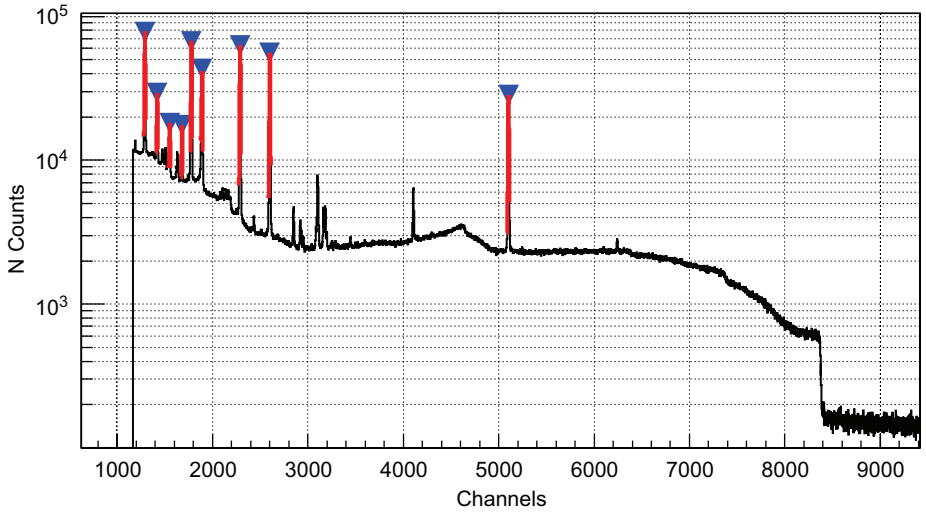

Fig. 5. Experimental spectrum of backscattered photons with calibration lines. 1 Channel = 0.512 keV.

The edge of the Compton spectrum is fitted with the six-parameter function:

$$g(x,p_{0\ldots5}) = \frac{1}{2}(p_2 + p_3(x-p_0)) \cdot \mathrm{erfc}\left[\frac{x-p_0}{\sqrt{2}p_1}\right] - \frac{p_1 p_3}{\sqrt{2\pi}} \cdot \exp\left[\frac{(x-p_0)^2}{2p_1^2}\right] + p_4 + p_5(x-p_0) \quad (7)$$

where the parameters are: p_0 is the edge position, p_1 the edge width, p_2 the edge height, p_3 the left slope, p_4 the background level, p_5 the background slope. The p_0 parameter gives an information about the average beam energy during the data acquisition period, while p_1 is mostly coupled with the beam energy spread. The edge of the Compton spectrum together with fit results is shown in Fig. 6. Parameters p_3, p_5 are free due to strong energy dependence of the absorption coefficient.

The statistical accuracy of the beam energy calculation is about 70–100 keV for a 1 h run. Its allows to determine a beam energy drift or jump at the level of 150 keV. For the beam energy spread the statistical error is about 1.4 times larger. This results in a 10% relative accuracy, which is not quite interesting. Averaging for longer period suffers from systematic errors which are being studied now.

3.2. Results

The result of each energy measurement is available for the on-line representation. Fig. 7 shows the beam energy history for one week in January 2007 near the τ production threshold. The

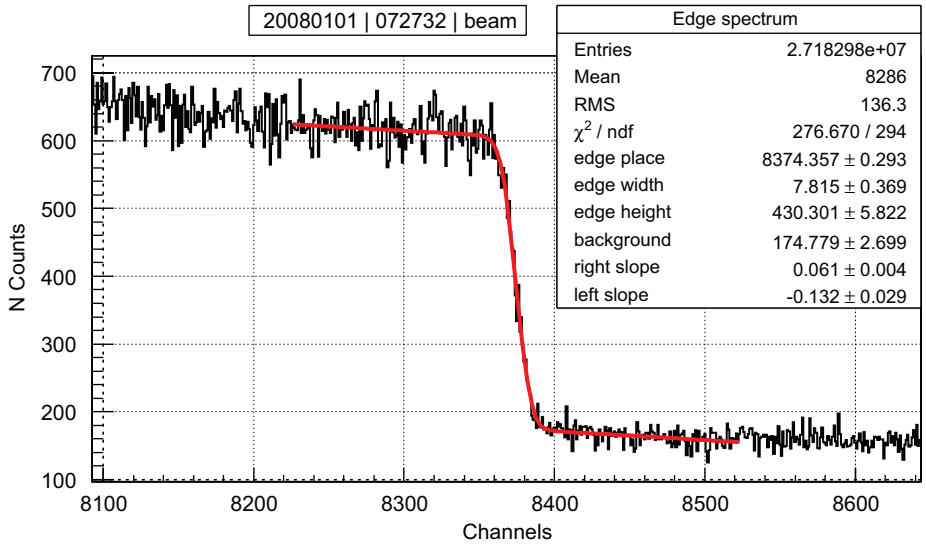

Fig. 6. Spectrum fragment near ω_{max}, Ebeam is about 1580 MeV, $\omega_{max} = 4.470$ MeV. Stat. error for E_{CBS} is 0.027 MeV.

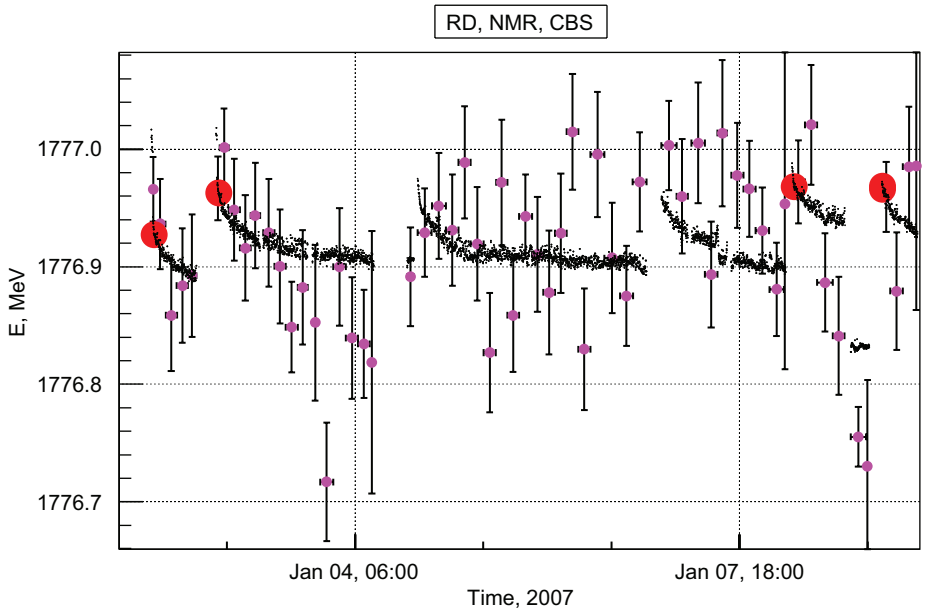

Fig. 7. Beam energy vs time for January 2007. Circles are obtained by RD, lines are for magnetic field approximation. Points with error are from the CBS monitor. A jump of 150 keV happened on January 8.

circles show RD energy measurements, lines show the beam energy interpolation from the magnetic field measurements—E_{NMR}. One can see the ~100 keV energy drift after guide field magnetization cycles. The points with errors show results of the CBS monitor. One can see a sudden energy jump which happened at the end of the week. After that the magnetization cycle was done for the energy adjustment.

3.3. Systematic errors

The absolute accuracy of the CBS monitor was checked by the comparison of its results with the RD when both measurements were done simultaneously. The systematic error of the CBS monitor has two main contributions.

3.3.1. Laser-beam optics

The VEPP4-M beam has an energy spread about 0.7 MeV for the beam energy of 1800 MeV. There is a correlation between a particle coordinate in an orbit plane and its energy. The scattered photons also carry energy-coordinate and energy-angle correlations. Thus a shift of a measured energy happens when:

- The center of HPGe detector is essentially shifted from the CBS spot. The same effect can be caused by a misplaced collimator of CBS photons.
- A center of laser spot is shifted from the beam center due to a beam movement or a laser optics instability, then $\Delta E_{CBS} \sim \sigma(E)(\sigma_x/\sigma^2_{spot})\Delta x$.

At the very beginning of the experiment the shift of $E_{CBS} - E_{RD}$ was reaching 0.5 MeV. To suppress these effects the following steps were done.

- The detector was moved closer to the interaction point and all collimators were removed.
- A laser spot size was increased.
- A feedback system was organized which periodically aims the laser beam to maximize the CBS rate.

All that helped to keep the maximum energy shifts below 100 keV level for a stable situation.

3.3.2. HPGe detector calibration

The available γ-sources allow to get photons with a maximum energy of 2750 keV. The calibration curve is a polynomial of 2nd or 3rd order degree. According to the tables [26] the energy of γ's are known with the accuracy of 2–15 eV. The actual accuracy of the γ peak position is limited by 0.010 keV due to the pile-up noise which changes peak shapes. Because of the scale nonlinearity the 0.010 keV calibration accuracy provides an error $\sigma(E) \sim 50$ keV during the extrapolation to ω_{max}. For a usual run this error is 4–5 times larger. To reduce this error, the RD measurements were used to determine nonlinearity terms for different periods. Then its fixed values are used for the energy calculation.

To avoid this problem for future applications it is planned to get a special source for 6.1 MeV γ-quanta.

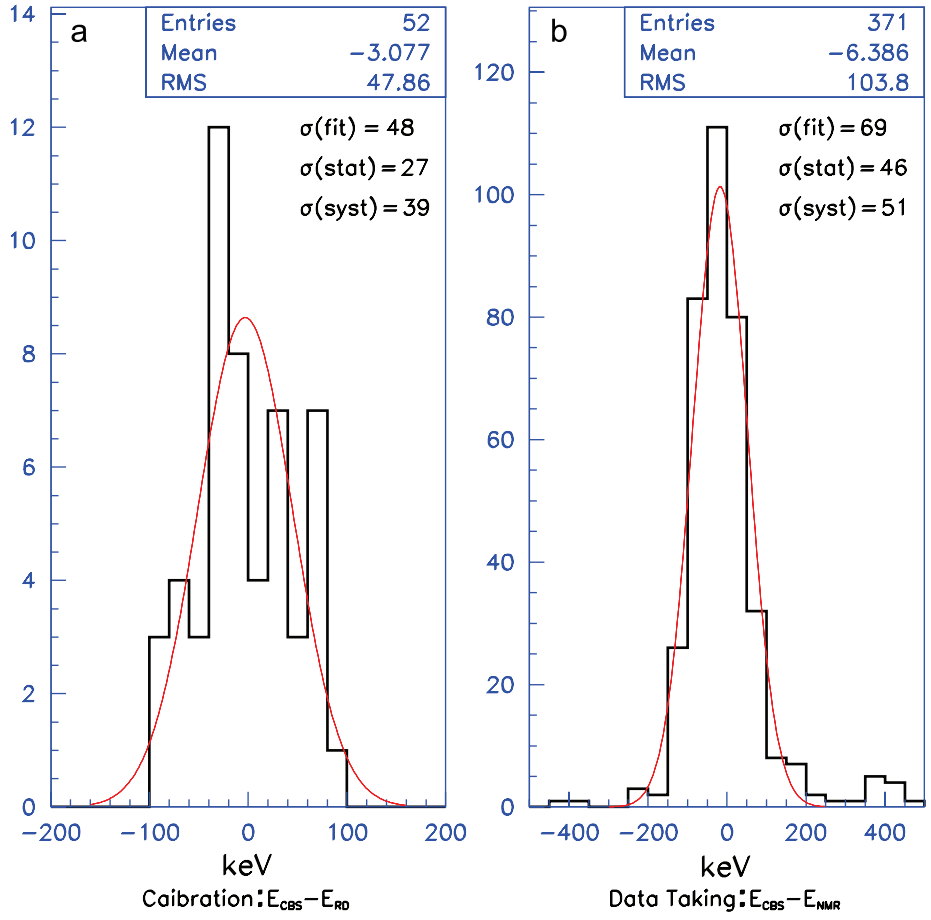

Fig. 8. Accuracy check of the CBS monitor with RD (a) and magnetic (b) measurements. The average statistical errors of the CBS measurements are 27 (a) and 46 (b) keV. Additional spreads are about 40 (a) and 50 (b) keV. Points in the right tail (b) indicate beam energy jumps or orbit movements.

3.3.3. Error estimation

At the present time the study of systematic errors is in progress. In practice errors are estimated separately for different time periods under an assumption: $\sigma^2_{\text{visible}} = \sigma^2_{\text{stat}} + \sigma^2_{\text{syst}}$.

The histogram in Fig. 8a shows the difference between CBS and RD measurements for simultaneous calibrations during a 2 month run near the τ production threshold. The additional spread is about 40 keV while the average statistical error is 27 keV. The beam energy for data taking between RD calibrations is estimated with the magnetic field measurements. Fig. 8b shows the plot of $E_{\text{CBS}} - E_{\text{NMR}}$ for the same period. The collection time for each CBS measurement is 2–3 h, the average statistical error is 45 keV. Additional spread is 50 keV. Points outside the peak indicate problematic runs when a large difference arises. In such cases the collider is forced to start a magnetization cycle to adjust the beam energy and prevent data spoiling.

4. Conclusion

At present time the KEDR detector at the VEPP-4M collider carries out a number of experiments for precise measurements of charmed mesons and τ lepton masses in the beam energy range $E = 1.5-1.9$ GeV. The resonant spin depolarization technique allows to measure instantaneous E with an accuracy of about 1–3 keV in special runs. For data taking some interpolation procedure is necessary. The resulting accuracy is 5–30 keV.

The Compton BackScattering monitor allows fast on-line monitoring of the collider energy with accuracy about 150 keV. The proper analysis provides an accuracy of $\sim$100 keV for for a 1 h measurement. The systematic error is 50–100 keV.

References

[1] V.V. Anashin, et al., Nucl. Instr. and Meth. A 478 (2002) 420.
[2] V.V. Anashin, et al., in: Proceedings of EPAC, vol. 1, 1998, p. 400.
[3] V.E. Blinov, et al., Nucl. Instr. and Meth. A 494 (2002) 81.
[4] N.Yu. Muchnoi, S.A. Nikitin, V.N. Zhilich, (Novosibirsk, IYF). in: European Particle Accelerator Conference (EPAC 06), Edinburgh, Scotland, 26–30 June, 2006, Published in "Edinburgh 2006, EPAC," pp. 1181–1183.
[5] A.D. Bukin, et al., in: Warsaw 1975, Proceedings, International Symposium on High Energy Physics, Dubna, 1975, pp. 138–147, Novosibirsk Inst. Nucl. Phys.—IYAF 75–64.
[6] A.N. Skrinsky, Yu.M. Shatunov, Sov. Phys. J. 32 (1989) 548.
[7] A.D. Bukin, et al., Yad. Phys. 27 (1978) 985 (in Russian).
[8] L.M. Barkov, et al., Nucl. Phys. B 148 (1979) 53.
[9] A.A. Zholentz, et al., Phys. Lett. B 96 (1980) 214.
[10] A.S. Artamonov, et al., Phys. Lett. B 118 (1982) 225.
[11] A.S. Artamonov, et al., Phys. Lett. B 137 (1984) 272.
[12] S.E. Baru, et al., Z. Phys. C 30 (1986) 551 (Erratum Z. Phys. C 32 (1986) 622.).
[13] W.W. MacKay, et al., Phys. Rev. D 29 (1984) 2483.
[14] D.P. Barber, et al., Phys. Lett. B 135 (1984) 498.
[15] L. Arnaudon, et al., Phys. Lett. B 307 (1993) 187.
[16] W.-M. Yao, Particle Data Group, et al., J. Phys. G 33 (2006).
[17] Ya.S. Derbenev, et al., Particle Accelerators, vol. 8, 1978, p. 115.
[18] A.E. Bondar, et al., in: Proceedings of the 12th International Conference on High Energy Acceleration, FNAL, Batavia, Illinois, 1983, p. 240.
[19] V.E. Blinov, et al., Nucl. Instr. and Meth. A 494 (2002) 81.
[20] S.I. Mishnev, et al., in: SPIN a 2000, 14th International Spin Physics Symposium, AIP, vol. 570, 2001, p. 892.
[21] V.E. Blinov, et al., Nucl. Instr. and Meth. A 494 (2002) 68.
[22] V.M. Aulchenko, et al., Phys. Lett. B 573 (2003) 63.
[23] K.Y. Todyshev, et al., KEDR Collaboration, PoS HEP 2005, 2006, p. 115.
[24] V.V. Anashin, et al., JETP Lett. 85 (2007) 347.
[25] R. Klein, et al., Nucl. Instr. and Meth. A 384 (1987) 293;
R. Klein, et al., Nucl. Instr. and Meth. A 486 (2002) 545.
[26] Lund Nuclear Data Service ⟨http://nucleardata.nuclear.lu.se⟩.